

---

# *DISCUSSION*

---

## 5. DISCUSSION

### 5.1. CHOOSING THE BEST POLYMER FOR THE PASSIVE CHEMICAL DOSING SYSTEM

The polymer films evaluated in Experiment I exhibited varying degrees of degradation when stored in urine over sixteen days. This degradation led to a decrease in the pH of the stored urine (Fig. 11). Polypropylene (PP) degradation under abiotic conditions results in the formation of carbonyls and hydroperoxides (Gewert et al., 2015). Polylactic acid (PLA) degrades through the hydrolysis of ester bonds in alkaline conditions, producing lactic acid and alcohol (Södergård & Stolt, 2002). Similarly, polycaprolactone (PCL), another polyester, degrades via hydrolysis of ester bonds, yielding 1,6-hexanediol and 6-hydroxycaproic acid (Leroux et al., 2020). Polyvinyl alcohol (PVOH) degradation in abiotic conditions generates ketones, fatty acids, and alcohols (Petkovšek et al., 2023). The acidic by-products from the degradation of these polymers contributed to the observed decline in urine pH over the storage period.

PVOH, the only water-soluble polymer tested in Experiment I, exhibited notable swelling 135% in CF 2 urine after 16 days (Fig 14 (a) and (b)) and the highest percentage degradation in terms of number average ( $M_n$ ) and weight average ( $M_w$ ) molecular weights, at 37% and 47%, respectively. This indicates a substantial breakdown of the polymer chains. The swelling of PVOH films is due to hydrogen bonding between the polymer's hydroxyl groups and water in urine, leading to osmotic pressure that attracts more water and eventually compromises the polymer's structural integrity, causing chain separation and dispersion (Harpaz et al., 2019). Despite this, PVOH does not completely degrade and can persist as microplastics for extended periods (Petkovšek et al., 2023). Weight loss of PVOH films was 15% in CF1 urine and 27% in CF2 urine after 16 days (Fig 14 (c) and (d)).

Among the polymer films assessed, PLA demonstrated the greatest weight loss (Fig 14 (c) and (d)). PLA degrades via hydrolysis, where water molecules diffuse into the polymer and cleave ester bonds, reducing swelling but accelerating degradation (Casalini et al., 2019). Despite having a similar structure to PLA, PCL showed lower weight loss, as PLA's carboxyl end groups autocatalyze degradation, causing faster internal surface degradation (Deka et al., 2023). PCL's lower hydrolytic degradation is attributed to its hydrophobicity and

crystallinity (Kodama, 2013). The degradation rate of polyesters is influenced by temperature, with higher temperatures increasing interactions between polymer chains and hydroxide ions (Deka et al., 2023). Consequently, PCL requires higher temperatures than PLA for comparable degradation. Polypropylene (PP), known for its chemical and solvent resistance at lower temperatures (Maddah, 2016), showed negligible weight loss (<5%) in urine.

Certain ions can engage in ion-exchange reactions with polyester functional groups, altering the polymer structure and facilitating degradation (Lee & Gardella, 2000). Salts and ions also affect the water sorption behaviour of polyesters, accelerating hydrolysis and other degradation mechanisms (Lee and Gardella, 2000). PLA films had 25% and 13% degradation for  $M_n$  and  $M_w$  respectively because of the hydrolysis of ester bonds by urine salts and ions despite minimal swelling. PLA degradation is influenced by pH and temperature (Deka et al., 2023), suggesting its potential use for encasing chemicals in source-separated urine and wastewater treatments at temperatures below 30°C for short durations. The degradation rate of PLA is also affected by its crystalline structure, with the less crystalline enantiomer PDLA degrading faster than the more crystalline PLLA under similar conditions (Vieira et al., 2010). Therefore, PLLA or PDLA can be utilized in passive dosage systems, with controlled chemical release depending on the selected enantiomer.

## **5.2. UNDERSTANDING THE EFFECTS OF pH, TEMPERATURE AND FILM THICKNESS ON THE DEGRADATION RATE OF POLY L-LACTIC ACID**

In Experiment II, the Degradation of PLLA in alkaline conditions proceeds via the hydrolysis of ester bonds, resulting in the formation of carboxylic acid and alcohol (Södergård & Stolt, 2002). This process breaks PLLA into soluble oligomers and monomers (Karamanlioglu et al., 2017), which, when retained in the medium, cause a decrease in pH (Fig. 12) (Zaaba & Jaafar, 2020). This accounts for the observed pH decline in alkalized fresh urine over time in this study. The self-catalyzing nature of hydrolysis accelerates the degradation rate and the associated pH reduction over time.

In the presence of cations or bases, PLLA degrades to form lactate salts, L-lactides, and L-methyl lactate (Avgoustakis, 2005). With the presence of  $\text{Ca(OH)}_2$ , L-methyl lactate can further form calcium lactate ( $\text{CaL}_2$ ) (Alberti et al., 2020). Three observations support the formation of  $\text{CaL}_2$  in Experiment II. First, there was a significant decrease in urine calcium concentration over time, with a 43% reduction in samples containing 0.05 mm PLLA at 20 °C (Fig. 27). Second, EDX analysis showed increased calcium content in the films (Fig. 28). Third, SEM images revealed numerous solid deposits on PLLA films in urine (Fig. 21). Furthermore, FT-IR spectra of PLLA films in  $\text{Ca(OH)}_2$  dosed urine exhibited broad peaks characteristic of lactate groups ( $1500\text{-}1300\text{ cm}^{-1}$  and  $800\text{ cm}^{-1}\text{-}650\text{ cm}^{-1}$ ) (Dippong et al., 2017), which were absent in Mili-Q water (Fig. 25).

Higher temperatures increase the molecular motion of PLLA chains and hydroxide ions, increasing the collision frequency and accelerating the hydrolysis of ester bonds (Tsuji & Nakahara, 2002). This was evident as degradation was more pronounced at 45 °C compared to 20 °C, correlating with a greater pH decrease in urine at the higher temperature ( $p < 0.001$ ). Molecular weight reductions were also more notable at 45 °C. Virgin PLLA is semi-crystalline, meaning it has both crystalline and amorphous regions. PLLA degrades in two stages: initially, hydrolysis occurs in the amorphous regions, increasing crystallinity, followed by degradation of the crystalline phase from the edges. This is consistent with PXRD results showing fewer crystalline peaks at 45 °C compared to 20 °C, and increased crystallinity in films stored at 20 °C compared to the virgin film (Fig. 15).

In neutral and acidic media, PLLA undergoes bulk erosion via chain end-scission (Teixeira et al., 2021). However, surface erosion via random ester bond cleavage predominates in alkaline conditions, accelerating degradation (Karamanlioglu et al., 2017). Hydroxide ions catalyze this process by nucleophilic attack on the ester carbonyl carbon, initiating bond cleavage (Tsuji & Nakahara, 2002). This was evidenced by greater visible degradation in films stored in  $\text{Ca(OH)}_2$  dosed urine compared to Mili-Q water (Fig. 17).

FT-IR curves of 0.05 mm PLLA films stored in Mili-Q water for eight days revealed new peaks, indicating hydrolytic scission of ester bonds. A broad peak at  $1500\text{ cm}^{-1}\text{-}1000\text{ cm}^{-1}$  suggests the presence of carboxylate groups, while peaks around  $3600\text{ cm}^{-1}\text{-}3500\text{ cm}^{-1}$  indicate increased  $\text{-COOH}$  and  $\text{-OH}$  bonds, signifying lactic acid formation (Fig. 24)

(Granados-Hernández et al., 2018). The increase in peaks around  $3000\text{ cm}^{-1}$  reflects higher methyl group content (methyl lactide) (Choksi & Desai, 2017).

Crystallinity ( $X_c$ ) of PLLA increased in films stored at  $45^\circ\text{C}$  in Mili-Q water, indicating degradation of the amorphous phase, which did not change at  $20^\circ\text{C}$ . This suggests faster degradation at higher temperatures. Molecular weights ( $M_n$  and  $M_w$ ) increased relative to the virgin film, likely due to the more rapid degradation of smaller fragments, which biases molecular weight calculations towards larger fragments (Makino et al., 1986).

### 5.3. BUFFERING THE pH OF THE DEHYDRATING ALKALINE URINE

Experiment III evaluated the efficacy of the PLLA-based passive chemical dosing system in maintaining a stable pH level of urine during alkaline urine dehydration. The passive chemical dosing system was engineered to enable the gradual release of encapsulated chemicals (KOH) within PLLA pouches, ensuring pH modulation without requiring active intervention. The results demonstrate that the release of KOH pellets from the pouches effectively sustains a safe pH level over an extended period.

The release time of encased KOH was found to be correlated to the number of PLLA pouch layers. In consistent environmental conditions (constant CF and pH), one-layer pouches were the first to rupture and release KOH pellets, followed sequentially by two-layer and three-layer pouches (Table S5 of SI). The data also showed that pouches in urine at pH 14 released KOH more rapidly than those in urine at pH 11, consistent with previous findings (Deka et al., 2023), indicating that the degradation rate of PLLA is a function of the pH of the medium.

Following the initial pH surge due to the KOH pellets, a gradual decline in urine pH was observed over subsequent sampling days (Table S4 of SI). This decline is attributed to the formation of lactic acid, which subsequently forms KLa. The pH of a 1-molar solution of lactic acid is approximately 3.5, while that of potassium lactate in neutral media is 7.45. Additionally, a minor pH decrease occurred just before the KOH pellets dissolved, due to the formation of lactic acid as the PLLA pouches began to degrade. However, this pH drop is minimal and would have negligible impact in practical applications. Upon calculation, it is estimated that  $9.9 \times 10^{-11}$  moles of LA are needed for the pH of 1L urine to drop from 12 to

10 and  $9.9 \times 10^{-11}$  moles of KOH would be necessary to raise the pH back to 12. Considering that degradation of PLLA in urine in only form LA ( $pK_a \approx 3.86$ ) and no amount of KLa or other Lactide salts are formed, 0.1 g PLLA (weight of a single layered pouch) would form approximately 0.00278 moles of LA while 0.2 g KOH (standard dosage in each pouch) has approximately 0.00357 moles of KOH.

The concentration of potassium in urine gradually decreased after the initial surge due to KOH pellets, attributed to the formation of KLa, which can be quantified as per Eq 11. Fig. 29 highlights that the highest amount of KLa after thirty-two days was observed in CF 10, pH 14 urine for two-layered and three-layered pouches, while the lowest amount was in CF 1, pH 11 urine for three-layered and two-layered pouches. This indicates the varying degradation mechanisms of PLLA under different CF and pH conditions in urine. Although three-layered pouches contain more PLLA than two-layered pouches, the two-layered pouches completely degraded after thirty-two days in CF 10, pH 14 urine, while the three-layered pouches only partially degraded, resulting in higher KLa formation in two-layered pouches. PLLA degrades more rapidly in higher CF and pH urine. This is further highlighted by the calculated KLa amounts in CF 1, pH 11 urine, where three-layered pouches formed the least KLa, followed by two-layered pouches after thirty-two days.

The pH of incoming urine to the drying cassette will be approximately 11, with a CF of 1. As dehydration commences, pH will gradually decrease due to carbonic acid formation (Simha et al., 2020). Single-layer pouches will rupture within two days, releasing the enclosed chemicals and raising the pH to safe levels. Although the formation of KLa results in a slight pH drop, this experiment conducted in 100 mL urine suggests the impact would be negligible in a drying cassette containing over 50 L of urine.

Three-layered pouches can stabilize the pH of dehydrating urine for up to one month, as evidenced by the results. The pouch layer thickness can be increased to 0.1 mm and 0.25 mm to extend this duration. Increasing the thickness to 0.1 mm from 0.05 mm can double the degradation time while increasing it to 0.25 mm can extend it up to five times (Deka et al., 2023). Consequently, the PLLA-based passive dosing system can be utilized to passively dose chemicals, stabilizing the pH of alkaline urine dehydration for up to five months.

The objective of the circular alkaline dehydrating setup in experiment IV was to assess its effectiveness in maintaining a safe pH level ( $>10$ ) during urine dehydration. The setup dehydrated alkaline urine to CF 5, an 80% reduction in the original volume. The maximum volume reduction was achieved during 12-hour drying cycles, resulting in a 92% decrease. In the linear setup, a steady decline in urine pH was observed regardless of the superabsorbent polymer (SAP) used with the final pH of CF 5 urine being 9.7 for KPAC and 9.65 for NaPAC (Fig. 31). This pH decrease was attributed to the absorption of  $\text{CO}_2$  from ambient air and the subsequent formation of carbonic acid (Simha et al., 2020).

In contrast, the circular system was designed to recycle air after it passed through absorption chambers, thereby minimizing the entry of ambient air and the formation of carbonic acid, thus preventing the urine pH from dropping below 10. The pH of CF 5 urine in the circular system was reported to be 11.65 for KPAC and 11.68 for NaPAC, which remained within the safe range (Fig. 31). Therefore, the circular system proved effective in maintaining a safe pH during the dehydration of alkaline urine.

However, the circular system exhibited a slower drying rate compared to the linear setup (Fig.32). The linear setup continuously exchanged humid air with fresh air, which had a higher moisture-absorbing capacity (William et al., 2015), while the circular system recycled humid air, relying on SAPs to remove moisture and absorb more. Consequently, the circular system required more time to dehydrate the same urine volume as the linear setup. Nevertheless, the drying rate of the circular system can be improved by optimizing the design of the absorption chambers to increase the interaction surface area between humid air and SAPs.

Stabilization and nutrient recovery from human urine can also be achieved through various other methodologies, each presenting distinct advantages and limitations. Electrochemical approaches facilitate chemical-free nitrification and nitrate recovery by maintaining pH stability and extracting nutrients, although they are energy-intensive and face scalability challenges (De Paepe et al., 2021). Air and  $\text{CO}_2$  bubbling techniques remove calcium from stabilized urine, mitigating scaling risks for advanced treatment processes while preserving nitrogen for nutrient recovery, but they necessitate the management of precipitated solids (Courtney et al., 2021a). Similarly, calcium removal via precipitation enhances reverse

osmosis efficiency by protecting membranes but increases system complexity (Courtney et al., 2021b). Electrochemical ammonia and urea removal utilizing IrO<sub>2</sub> electrodes demonstrates potential for pollutant reduction, although carbonates diminish efficiency, and the focus is primarily on wastewater treatment rather than nutrient recovery (Amstutz et al., 2012).

#### 5.4. EXTRACTING REUSABLE WATER

Experiment IV evaluated the possible application of commercially available potassium polyacrylate (KPAC) and sodium polyacrylate (NaPAC) in extracting reusable water from urine and removal of organic metabolites. For each 12-hour drying cycle, 100 g of SAP was evenly divided between two chambers (50 g per chamber). The average moisture absorption capacity of KPAC was 85.6%, while NaPAC's was 83.5% across eight cycles (Fig. 34). When KPAC and NaPAC were mixed in a 1:1 ratio, the average absorption was 85.5%. The moisture absorption capacity of the SAPs in the circular setup is influenced by the surface area of interaction between the SAPs and humid air (494 cm<sup>2</sup> total, 247 cm<sup>2</sup> per box) (Kalinowski & Woyciechowski, 2019). The initial absorption rate (first cycle) of KPAC was 0.05 kg/day/m<sup>2</sup>, compared to 0.043 kg/day/m<sup>2</sup> for NaPAC, a difference likely due to the structural differences between the SAPs (Ma et al., 2019). NaPAC is finer, while KPAC is coarser. The SAPs expand and crosslink, forming a gel-like layer on top (Ma et al., 2019). Finer NaPAC particles bond more closely, reducing interaction with moist air and resulting in a lower drying rate for the circular system when NaPAC is used. The average drying rate of the circular system with NaPAC was 0.0008 kg/day/m<sup>2</sup>, while with KPAC it was 0.00087 kg/day/m<sup>2</sup>. The drying rate for CF 1.25 to CF 2 urine was 0.0011 kg/day/m<sup>2</sup> for KPAC and 0.0009 kg/day/m<sup>2</sup> for NaPAC. The mixed SAP performed similarly to KPAC, with an initial absorption rate of 0.0043 kg/day/m<sup>2</sup>.

After the fourth cycle, the absorption percentage of the SAPs decreased, remaining above 90% for KPAC and the 1:1 mixture and 85.6% for NaPAC. By the eighth cycle, the absorption rate decreased to 70% for KPAC, 69.5% for NaPAC, and 65% for the mixed SAP, attributed to SAP degradation from repeated heating during dehydration. Thermal degradation of polyacrylates forms smaller molecular-weight polyacrylates, acrylic acid, and other low



molecular-weight organic compounds (Czech et al., 2015). FT-IR curves of the SAPs after the eighth cycle indicate new peak formation. The peak around  $3000\text{ cm}^{-1}$  indicates a shift in existing  $-\text{CH}_3$  bond stretching, suggesting a reduction in molecular weight (Lavrič et al., 2021). Peaks around  $1750\text{ cm}^{-1}$  and  $1400\text{ cm}^{-1}$  are due to  $\text{C}=\text{O}$  stretching and  $-\text{CH}_3$  or  $-\text{CH}_2$  bending, signifying the formation of acrylic acid (Feng et al., 2018). Despite SAP degradation, water extraction efficiency remained over 90% for all SAPs except in the eighth cycle for NaPac and the mixed SAP, which were 87.5% and 88.8%, respectively.

Recent advancements in atmospheric water extraction (AWE) technologies elucidate a variety of techniques, methodologies, quantified findings, and associated challenges. Mishra and Patel (Mishra and Patel., 2021) categorized AWE methods into passive and active techniques. Passive dew collection utilizes radiative cooling surfaces to condense atmospheric moisture, achieving collection rates of  $0.3\text{--}1.5\text{ L/m}^2/\text{day}$  under optimal humid conditions, although efficiency significantly decreases in arid environments. Desiccant-based systems employ hygroscopic materials such as silica gel or lithium chloride to absorb water, followed by thermal desorption, enabling water recovery rates of  $50\text{--}80\%$  depending on material type and humidity levels. However, thermal energy requirements pose a limitation for scalability. Active methods such as cooling-based condensation achieve higher yields of up to  $10\text{ L/day/kW}$  but are constrained by high energy demands and climatic dependency, particularly in regions with low humidity.

Siddiqui and colleagues (Siddiqui et al., 2022) investigated membrane-based technologies and solar-powered systems. Membrane-based approaches, utilizing hydrophobic or superhydrophilic materials, facilitate selective moisture capture with recovery rates ranging from  $3$  to  $5\text{ L/m}^2/\text{day}$ , contingent upon the design and environmental conditions. Solar-powered condensation systems incorporate photovoltaic energy or solar thermal heat for sustainable operation, yielding up to  $8\text{ L/day}$  under optimal sunlight exposure. While these systems reduce dependence on external power sources, high initial costs and efficiency losses in cloudy or shaded conditions present challenges for large-scale deployment.

Kandael and colleagues (Kandael et al., 2022) reviewed advancements in adsorption-based and hybrid systems. Adsorption systems employing advanced materials such as metal-organic frameworks (MOFs) or zeolites demonstrated significant potential, achieving up to

0.5–1.0 L/day/kg of material, even in arid climates with relative humidity as low as 20%. Hybrid systems combining condensation and desiccant regeneration further enhanced water collection efficiency by 20–40% compared to standalone methods. Despite these improvements, challenges persist, including the durability of adsorption materials, energy-intensive desorption processes, and the cost of advanced materials.

Across these studies, AWE technologies demonstrate significant potential for augmenting traditional water supplies, particularly in water-stressed regions. However, substantial challenges persist, including energy efficiency, material costs, climatic dependency, and system scalability. Addressing these limitations through material innovation and integration of renewable energy sources is essential for widespread adoption.

### **5.5. REMOVAL OF ORGANIC METABOLITES BY SAPs**

Approximately 50% of the organic micropollutants (OMs) that were tested for and detected in urine samples were removed (below the limit of detection) in the extracted water. Non-volatile and high molecular weight compounds, such as polypeptides, amino acids, nucleosides, and nucleotides, likely did not evaporate (Võ & Morris, 2014) and were absent in the moisture absorbed by SAPs. Low-molecular-weight, volatile, and water-soluble OMs needed to be removed by SAPs or activated carbon treatment. 40 out of 108 detected OMs had concentrations reduced by over 80% in recycled water. KPAC and NaPAC are anionic due to the carboxylate group ( $-\text{COO}^-$ ) (Yu et al., 2021), carrying a slight negative charge, especially when they absorb moisture. Through electrostatic attraction, they can adsorb positively charged OMs (Tiraferri & Elimelech, 2012). Positively charged OMs removed from the extracted water include Hippuric acid, Creatinine, 5-Oxoproline, Phenylacetylglutamine, Creatine, and 16 others. These OMs carry positive charges due to groups such as amino ( $-\text{NH}_3^+$ ) (Tiraferri & Elimelech, 2012), guanidinium ( $-\text{NH}=\text{C}(\text{NH}_2)^+$ ) (Hannon & Anslyn, 1993), quaternary ammonium ( $-\text{NR}_3^+$ ) (Li et al., 2023), imidazolium ( $-\text{C}_3\text{H}_3\text{N}_2^+$ ) (Tolomeu & Fraga, 2023) or polyamine (Agostinelli, 2020). Polyacrylates can also adsorb non-polar OMs via hydrophobic interactions (Xiao et al., 2020). Of the 219 OMs detected in urine, 123 were non-polar. Anionic polymers with porous structures can physically exclude larger OMs, acting as molecular filters (Yu et al., 2022).

## 5.6. REMOVAL OF ORGANIC METABOLITES BY ACTIVATED CARBON

Activated carbon can remove OM<sub>s</sub> through adsorption (Pourhakkak et al., 2021), chemisorption (Agboola & Benson, 2021), pore-size exclusion (Yu et al., 2024), and surface chemistry (Snoeyink & Weber, 1967). Adsorption works due to the physical adherence of OM<sub>s</sub> to the surface of the activated carbon. The large surface area and porous nature of activated carbon make it particularly effective for this purpose. During adsorption, OM<sub>s</sub> are attracted and held onto the carbon's surface, which reduces their concentration. This method can remove a broad range of OM<sub>s</sub>. Chemisorption involves a chemical reaction between the OM molecules and the surface of the activated carbon. Unlike physical adsorption, which is reversible, chemisorption forms a strong, often covalent bond, making it a more permanent solution for OM removal. This process can be highly selective, targeting specific OM<sub>s</sub> based on their chemical properties. Pore-size exclusion is a filtration mechanism that depends on the size of the pores in the activated carbon. OM<sub>s</sub> are physically excluded from passing through the carbon if they are larger than the pores. This method is particularly useful for removing larger organic molecules that cannot penetrate the fine pore structure of the activated carbon. Surface chemistry refers to the interactions between the surface of activated carbon and organic matter (OM) molecules. Various factors, such as the presence of functional groups on the carbon's surface, its acidity or basicity, and the overall chemical environment, can significantly impact the efficiency of OM removal. Although the study did not assess the impact of SAPs degradation on OM removal, it is a crucial aspect to consider in future research. SAPs, which are used for moisture absorption, could potentially release degradation products that might interact with OM<sub>s</sub> in water. Exploring these interactions and their implications for OM removal could further enhance the efficiency and applicability of SAPs when used in conjunction with activated carbon for comprehensive water treatment solutions. Thirteen OM<sub>s</sub> were removed (below the limit of detection), while five had concentrations reduced by over 80% after treatment with activated carbon. The impact of SAP degradation on OM removal was not evaluated in this study.

## 5.7. ENERGY DEMAND AND DESIGN OF THE CIRCULAR URINE DEHYDRATING SYSTEM

In examining the energy demands of a urine dehydration system, it is essential to consider both the thermodynamics of the system and the specific energy requirements. The lab-scale setup involved evaporating 50 g of urine using a pump rated at 200 watts and absorbing the moisture generated using superabsorbent polymers (SAPs) as desiccants. The pump consumed 8640 kJ of energy during every 12-hour drying cycle. The radius and height of the drying chamber were 6.25 cm and 16 cm, respectively, and the area of the drying surface was 0.14 m<sup>2</sup> square meters. The diameter of the connecting hoses was 12 mm, and the airflow rate was 35.316 m<sup>3</sup>/h. The total area of interaction between the SAPs and the moist air was approximately 500 cm<sup>2</sup>.

Scaling up the circular urine dehydration system would require significant design changes. Assuming the system can dehydrate urine generated by a family of four, the drying rate of the system should be around 6 L per day (1.5 L of urine per day per person). A 6.5 cm radius and 50 cm height dehydrating chamber can accommodate 6 L of urine. However, since the setup will be drying urine continuously, it will not be full or overflow. In the lab setup, the SAPs absorbed more than 90% of the moisture generated during every cycle of urine dehydration. Assuming that the SAPs absorb five times their weight in moisture and can last five dehydrating cycles before saturation, each chamber should accommodate around 80 L of swelled-up SAPs (10 L of buffer volume). Keeping the design, the same as the lab scale setup, there would be two absorption chambers with a 22 cm radius and 50 cm height (height similar to the dehydrating chamber). The combined interaction area between moist air and SAPs is estimated to be approximately 1.43 m<sup>2</sup>. It is essential to maintain a consistent and uninterrupted airflow rate to prevent significant drops in the system. To ensure portability and ease of cleaning, the diameter of the connecting pipe should be around 5 cm. To effectively dehydrate 5.4 kg of urine per day, the airflow rate should be 700 m<sup>3</sup>/h, which requires a minimum pump power rating of 500 W. The total energy consumption for dehydrating 5.4 kg of urine per day is 14,000 kJ (see detailed calculations in SI units). While a higher-rated pump may result in faster drying, it will also increase energy demand.

The efficiency of the lab-scale setup was extremely low at  $\eta = 0.012$ , with heat losses occurring through conduction (chamber walls), convection (connecting hoses), and radiation (pump). To improve the efficiency of the scaled-up setup, various design changes are necessary to minimize energy losses. The dehydrating chamber can be made from glass fiber-reinforced plastic, which has a low coefficient of thermal conductivity (0.18–0.3 W/mK) (Röchling, n.d) and excellent strength and corrosion resistance (Sathishkumar et al., 2014). However, this material can be costly due to the specialized equipment required for manufacturing (Sathishkumar et al., 2014). The absorption chambers can be made from polymers such as polypropylene or polycarbonate, which are strong, thermally insulating, easily moldable, and affordable (Shubhra et al., 2013) (Morgan & O'Neal, 1976).

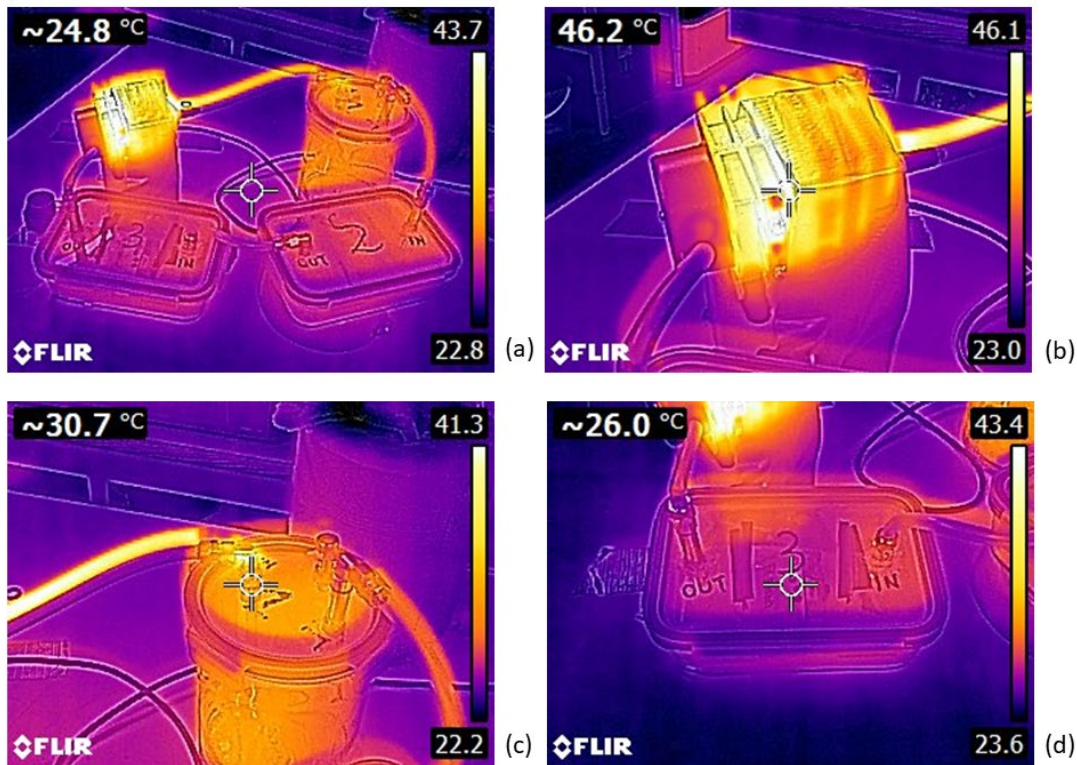


**Figure 36:** Thermal images of the circular alkaline urine dehydrator captured with FLIR E-series thermal camera. (a) ambient temperature of the close-loop urine dehydrating setup, (b) temperature of the 200W pump, (c) temperature of the dehydration chamber, (d) temperature of the absorption chamber containing SAPs.

To further enhance the efficiency of the urine dehydrating setup, several other strategies can be employed:

1. **Insulated Enclosure:** Placing the entire system in an insulated box can minimize heat loss to the environment, maintaining higher internal temperatures.
2. **Optimize Heating:** Efficient Heating Systems: Ensure the pump or heating element operates at optimal efficiency. Consider integrating a solar heating system to leverage renewable energy, reducing dependency on electrical power.
3. **Targeted Heating:** Direct heat specifically towards the urine to maximize the energy used for evaporation.
4. **Optimized Air Circulation:** Enhance airflow within the chamber to ensure uniform temperature and humidity distribution. This can reduce the energy required to maintain desired conditions.
5. **Ventilation Control:** Use variable-speed fans or automated vents to regulate airflow based on real-time humidity and temperature data.
6. **Moisture Control via Enhanced SAPs:** Develop superabsorbent polymers with higher moisture absorption rates. Increasing the surface area of SAPs can also enhance their efficiency in removing moisture from the air.
7. **Pre-Treatment of Air:** Use desiccant materials to pre-treat the air entering the system, reducing the initial humidity load.
8. **Sensor-Based Pump Operation:**
  - 8.1. **Moisture Sensors:** Equip the pump with sensors to monitor humidity levels. The pump can be programmed to operate only when necessary, preventing unnecessary energy consumption and overheating.
  - 8.2. **Temperature Sensors:** Integrate temperature sensors to ensure the system operates within optimal thermal ranges.
9. **System Design Optimization:** Chamber Size and Configuration: Evaluate and adjust the size and layout of the drying chamber to enhance heat and moisture distribution. A more compact design with optimized airflow paths can improve efficiency.
10. **Material Selection:** Use materials with lower thermal conductivity for the chamber walls to reduce heat loss.

## 5.8. OPTIMAL MANAGEMENT OF pH IN ALKALINE URINE DEHYDRATION

The two approaches that were discussed in the thesis have their pros and cons and are suitable for different scenarios. PLLA pouches for passive chemical dosing release alkaline chemicals (KOH) gradually, ensuring a steady pH level over an extended period without requiring frequent intervention. The pouches are made from biodegradable polymers which degrade into non-toxic byproducts such as lactic acid, making the system environmentally friendly. The release rate of chemicals can be controlled by adjusting the thickness and number of layers of the pouches, allowing for customization based on specific needs. It is a passive system that doesn't require active user involvement, making it user-friendly and reducing the need for maintenance. Besides buffering pH, these pouches can be used to administer other additives like peroxides to break down organic micropollutants and pathogens in urine.

However, The degradation rate of PLLA can vary significantly with temperature, pH, and ionic strength of the urine, which may lead to inconsistent performance in different conditions. There can be a slight decline in pH over time due to the formation of lactic acid from the degradation of PLLA, which may need to be counteracted. The use of biopolymers and controlled release systems might increase material costs. Fabricating the pouches with precise characteristics (thickness, layers) requires careful manufacturing processes, which might be complex and costly.

The circular alkaline dehydration setup prevents the entry of CO<sub>2</sub>, thereby avoiding pH drops due to carbonation, which enhances the stability of the pH level. The setup uses a heat pump-like mechanism to recycle energy, maintaining a constant temperature and reducing overall energy consumption. The use of SAPs effectively dehumidifies the air, promoting efficient urine dehydration and recycling of water for various applications. The circular system requires less frequent intervention to maintain pH levels, making it more convenient for long-term use.

But, circular setup is more complex and requires careful design and maintenance, which might be challenging to implement in all settings. The initial setup and equipment costs for the circular system are likely higher compared to PLLA pouches. The setup would require a continuous energy supply, which may not be feasible in all locations, unless solar energy is

used. Scaling up the circular- system for larger volumes of urine might present additional challenges and costs. The system relies on mechanical components like pumps and absorbers, which are prone to failures and require regular maintenance.

Talking about the feasibility of both the approaches, the PLLA pouches would be Ideal for households or small communities where the volume of urine to be treated is relatively low, making the gradual release and passive nature of PLLA pouches effective and manageable. These can also be used in portable toilets or temporary sanitation facilities (e.g., during events, construction sites) where a biodegradable and low-maintenance solution is advantageous and desirable. These pouches would be particularly useful in developing regions where access to complex machinery and continuous energy supply may be limited, but there is a need for effective and environmentally friendly urine treatment. The circular setup would be suitable for urban areas with access to a reliable energy supply, where the circular- system can be maintained efficiently and where there is a need to handle larger volumes of urine. It would also be ideal for institutions such as schools, hospitals, and office buildings, where the system's capacity to handle significant volumes and its pathogen inactivation capability are advantageous. This setup will also be appropriate for permanent installations where the initial higher setup cost can be justified by long-term benefits. And finally, this setup can be a game-changer for informal settlements where there is a lack of proper sanitation systems and water, given that is using solar energy for dehydration and circulation of the air.

## **5.9. TECHNO-ECONOMIC ANALYSIS**

A techno-economic analysis of alkaline urine dehydration utilizing polymer-based solutions necessitates the evaluation of technical feasibility, economic viability, environmental impact, and regional applicability (Mahmud et al., 2022). Technical feasibility encompasses the assessment of the scalability of the circular alkaline dehydration setup, with emphasis on the utilization of superabsorbent polymers (SAPs) and polymer films for pH buffering and moisture absorption under local climatic conditions. For instance, factors such as India's elevated temperatures or Sweden's low temperatures could influence the degradation rates of polymer films and the moisture recovery efficiency of SAPs.



Economic viability requires comprehensive cost analyses, including capital expenditures for infrastructure and polymer procurement, operating expenses for maintenance, and energy costs for recycling processes. Revenue generation through the sale of nutrient-rich fertilizers and recycled water for agricultural applications can offset these costs (Kabdaşlı & Tünay, 2018). Comparatively, Sweden's advanced systems may support higher initial costs with more energy-efficient designs, whereas India's adoption may prioritize cost-effective materials and processes. Environmental and social benefits must also be evaluated, particularly the reduction in nutrient pollution and the energy savings achieved by diverting urine from conventional wastewater treatment facilities to resource recovery systems. This aligns with circular economy principles, offering significant sustainability advantages in both regions (Udert & Wächter, 2012). From a social perspective, decentralized systems could enhance sanitation access in rural India while also providing opportunities for local employment.

Barriers and risks encompass regulatory challenges, such as compliance with fertilizer safety standards, and adoption barriers including cultural resistance to utilizing urine-derived fertilizers (Bischel et al., 2015). The integration of these systems into existing policies necessitates stakeholder engagement and training initiatives to ensure acceptance. A comparative analysis between India and Sweden points out the differences in energy use, material costs, and climate impacts. Sweden's systems benefit from high energy efficiency and advanced technology, while India's solutions may require adaptation for affordability and local resource availability. Additionally, financial metrics, including net present value (NPV), internal rate of return (IRR), and payback period, are essential for evaluating economic sustainability, with scenario analyses addressing uncertainties in material costs and market adoption rates. Collectively, these evaluations provide a comprehensive framework for determining the scalability and applicability of polymer-based urine dehydration systems, contributing to sustainable water and nutrient management on a global scale.